Acta Crystallographica Section F
Structural Biology and Crystallization Communications
ISSN 1744-3091

Crystallization and preliminary X-ray diffraction of human interleukin-7 bound to unglycosylated and glycosylated forms of its α-receptor

Joseph Wickham Jr and Scott T. R. Walsh*

Department of Molecular and Cellular Biochemistry, Comprehensive Cancer Center, Ohio State University, 467 Hamilton Hall, 1645 Neil Avenue, Columbus, OH 43210, USA

Correspondence e-mail: walsh.220@osu.edu

Received 25 July 2002
Accepted 1 September 2007

The interleukin-7 (IL-7) signaling pathway plays an essential role in the development, proliferation and homeostasis of T and B cells in cell-mediated immunity. Understimulation and overstimulation of the IL-7 signaling pathway leads to severe combined immunodeficiency, autoimmune reactions, heart disease and cancers. Stimulation of the IL-7 pathway begins with IL-7 binding to its α-receptor, IL-7Rα. Protein crystals of unglycosylated and glycosylated complexes of human IL-7–IL-7Rα extracellular domain (ECD) obtained using a surface entropy-reduction approach diffract to 2.7 and 3.0 Å, respectively. Anomalous dispersion methods will be used to solve the unglycosylated IL-7–IL-7Rα ECD complex structure and this unglycosylated structure will then serve as a model in molecular-replacement attempts to solve the structure of the glycosylated IL-7–α-receptor complex.

1. Introduction

Interleukin-7 (IL-7) is a cytokine with fundamental roles in extracellular matrix remodeling and in the development, proliferation and survival of T cells (in both humans and mice) and B cells (in mice) (Sfikakis & Tsokos, 1995; Fry & Mackall, 2002; Khaled & Durum, 2003; Ji, 2006; Ma *et al.*, 2006). IL-7 belongs to the common γ-chain receptor (γ_c) family of short-chain four-helix bundle interleukins including IL-2, IL-4, IL-9, IL-15 and IL-21 (Ozaki & Leonard, 2002). IL-7 functions through a stepwise cytokine-induced receptor heterodimerization mechanism. IL-7 first interacts with the extracellular domain (ECD) of its own membrane-bound receptor, IL-7Rα, forming a stable 1:1 IL-7–IL-7Rα assembly. Subsequently, the membrane-bound γ_c interacts with the intermediate 1:1 IL-7–IL-7Rα complex through its own ECD, forming the active ternary complex. The merger of the two cytokine receptors by IL-7 orients the cytoplasmic domains of the receptors so that their associated kinases (Janus and phosphatidylinositol 3-kinases) can phosphorylate sequence elements on the cytoplasmic domains (Jiang *et al.*, 2005). Transcription activators (signal transducers and activators of transcription, STATs and SRCs) bind to the phosphorylated sequence elements of the cytokine receptors, become phosphorylated, dissociate from the cytokine receptors, oligomerize and localize to the nucleus to elevate transcription (Jiang *et al.*, 2005).

The IL-7 pathways must be highly regulated for normal cellular function. Understimulation of IL-7-regulated pathways owing to mutations in the IL-7Rα ECD results in a form of severe combined immunodeficiency (SCID) characterized by no T-cell development in both humans and mice (Grabstein *et al.*, 1993; Puel *et al.*, 1998; Ponda *et al.*, 2006) and no B-cell development in mice (Grabstein *et al.*, 1993). At the other end of the spectrum, overstimulation of IL-7-regulated pathways results in the following medical problems: (i) allergic responses such as rheumatoid arthritis, acute rheumatic fever and chronic rheumatic heart disease (Watanabe *et al.*, 1998; Harada *et al.*, 1999), (ii) atherosclerosis of the arteries, leading to coronary artery disease (Woldbaek *et al.*, 2002; Damas *et al.*, 2003), and (iii)

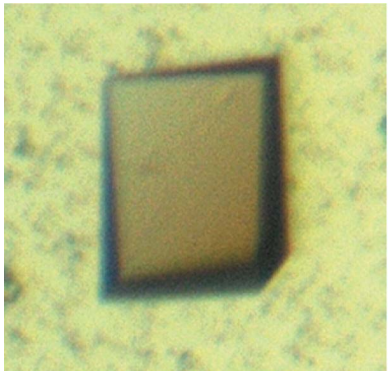

proliferation of chronic lymphophatic and acute myelogeneous leukemia cells (Digel *et al.*, 1991; Merle-Beral *et al.*, 1993; van der Plas *et al.*, 1996).

Human IL-7 (152 residues) is the largest glycoprotein in the γ_c family by more than 30 amino acids and shares less than 19% protein-sequence identity with the other interleukins in the γ_c family (Cosenza *et al.*, 2000). Human, but not mouse, IL-7 contains an insertion of 18 amino acids encoded by an additional exon (Lupton *et al.*, 1990). This exon insertion is predicted to be localized in the second crossover loop of IL-7 and has been shown by mutagenesis and cell-proliferation studies to be functionally inconsequential (Lupton *et al.*, 1990). The γ_c interleukins contain a variable number of cysteine residues involved in disulfide bonds (Ozaki & Leonard, 2002). A disulfide-bond mapping study of IL-7 identified three disulfide bonds to be formed by the six cysteine residues (Cosenza *et al.*, 1997). N-linked glycosylation of the three potential IL-7 sites was deemed to be biologically insignificant by bacterial expression of unglycosylated protein and cell-proliferation assays (Morrissey *et al.*, 1989; Goodwin *et al.*, 1989).

The full-length IL-7Rα is a 439-residue single-pass transmembrane glycoprotein consisting of three domains: a 219-residue ECD, a 25-residue transmembrane domain and a 195-residue cytoplasmic domain. The IL-7Rα ECD belongs to the cytokine receptor homology class 1 (CRH1) family, consisting of two fibronectin type III (FNIII) domains with three potential disulfide bonds in the N-terminal FNIII domain and a WS*X*WS primary sequence motif in the C-terminal domain (Bazan, 1990). The IL-7Rα ECD also shares less than 19% sequence identity with other ECDs in the γ_c family and contains six potential N-linked glycosylation sites. In humans, a splice variant of the ECD of the receptor has been isolated (Goodwin *et al.*, 1990; Levine, 2004). The biological function of this splice variant is unknown, but it has been postulated to bind and 'soak up' secreted soluble IL-7 and may modulate the IL-7 pathway both systemically and in localized immune responses (Goodwin *et al.*, 1990; Levine, 2004).

IL-7Rα also acts as the activating receptor when it binds the complex of thymic stromal lymphopoietin (TSLP) and its receptor, TSLPR. Activation of the TSLP signaling pathway triggers $CD4^+$ and dentritic cell proliferation in humans (Pandey *et al.*, 2000; Rochman *et al.*, 2007) and B-cell development in mice (Leonard, 2002; Pandey *et al.*, 2000). The protein-sequence identity between human IL-7 and TSLP and among the ECDs of IL-7Rα, TSLPR and γ_c is less than 15% (Leonard, 2002). Such low sequence homology makes structural studies crucial in deciphering the cross-reactivity nature of these cytokines and receptors.

Homology models based on the human growth hormone–receptor ternary complex (de Vos *et al.*, 1992) and the IL-4–IL-4Rα ECD (Hage *et al.*, 1999) structures have been reported for IL-7 or its associated complexes with IL-7Rα and γ_c (Kroemer *et al.*, 1996, 1998; Kroemer & Richards, 1996; Cosenza *et al.*, 2000). However, no atomic resolution structures of free IL-7, IL-7Rα ECD or their associated complexes have been determined by either NMR spectroscopy or X-ray crystallography. To fill these gaps in structural and functional information, we developed bacterial and insect-cell expression systems for IL-7 and IL-7Rα ECD. Because the native protein did not yield crystals diffracting to atomic resolution, we mutated residues in the loops of IL-7 to reduce surface entropy and promote favorable crystal contacts (Derewenda, 2004; Cooper *et al.*, 2007). IL-7 mutants resulting from this surface-loop entropy-reduction strategy yielded atomic resolution data sets for the unglycosylated and glycosylated complexes. Crystal structures of the IL-7–IL-7Rα ECD unglycosylated and glycosylated complexes will provide the structural framework needed to understand normal and aberrant IL-7 signaling.

2. Materials and methods

2.1. Protein purification and expression

Plasmids encoding the genes for human IL-7 and the full-length IL-7Rα were purchased from the American Type Cell Culture. For bacterial expression, the IL-7 gene (residues 1–152; Expasy code P13232) was cloned into the *Nco*I and *Bam*HI restriction sites of the expression vector pET-15b (Novagen). This IL-7 construct contains an extra Met-Gly at the beginning of the sequence. The ECD of IL-7Rα (residues 1–219; Expasy code P16871) was cloned into the *Nde*I and *Bam*HI restriction sites of pET-15b incorporating an N-terminal polyhistidine tag (HT) followed by a thrombin protease cleavage site (IL-7Rα-HT). This IL-7Rα ECD construct contains Arg-Ser-$(His)_6$-Ser-Ser-Gly-Leu-Val-Pro-Arg-Gly-Ser-His-Met-Glu at the N-terminus compared with the wild-type receptor. After thrombin protease cleavage of the His tag, IL-7Rα ECD has a Gly-Ser-His-Met at the N-terminus. The IL-7Rα ECD also contained an isosteric mutation of I118V compared with the protein sequence in the database.

Both wild-type (wt) IL-7 and IL-7Rα ECD expression vectors were transformed and expressed in *E. coli* cell line BL21(DE3) CodonPlus RP (Stratagene). Cells were grown to an OD_{600} of 0.8–1.0, induced with 0.5 m*M* IPTG and grown for an additional 3 h at 310 K. IL-7 and IL-7Rα ECD were expressed as insoluble inclusion bodies. Expressed proteins were extracted from cells by lysozyme treatment followed by disruption by sonication. Inclusion bodies of either IL-7 or IL-7Rα were first washed with 50 m*M* Tris–HCl pH 8.0, 5 m*M* EDTA and 2% deoxycholate to remove the cellular membranes, followed by washes with water to remove traces of the detergent. Washed inclusion bodies were solubilized in 5 *M* guanidine hydrochloride (GdnHCl), 50 m*M* Tris–HCl pH 8, 50 m*M* NaCl and a 10:1 molar ratio of reduced:oxidized glutathione. Refolding of the proteins was achieved by a ninefold dilution at 277 K overnight into buffer without GdnHCl but with 0.1 *M* arginine to allow the proper refolding and formation of disulfide bonds.

The refolded solution containing IL-7 was concentrated and dialyzed twice against 4 l of 5 m*M* sodium hydrogen phosphate pH 7.0, 75 m*M* NaCl at 277 K. IL-7 was purified on a Source S (GE Healthcare) cation-exchange column equilibrated in the same buffer. IL-7 was eluted from the column using a gradient from 75 m*M* to 1 *M* NaCl. Fractions of IL-7 were concentrated and purified on a Sephacryl S-200 (26/60, GE Healthcare) size-exclusion chromatography column equilibrated with TBS buffer (10 m*M* Tris–HCl pH 7.4, 150 m*M* NaCl). Mass spectrometry confirmed the molecular weight and the formation of the three disulfide bonds. Protein yields for wt IL-7 from *E. coli* were approximately 5 mg per litre of culture.

Refolded IL-7Rα ECD was loaded directly onto a cobalt-affinity column (Talon, Clonetech) equilibrated in buffer *A* (50 m*M* sodium phosphate pH 7.2, 0.3 *M* NaCl, 10 m*M* imidazole). Nonspecific proteins were washed away by further treatment with buffer *A*. IL-7Rα was eluted from the column with buffer *B* (50 m*M* sodium phosphate pH 7.2, 0.3 *M* NaCl, 0.15 *M* imidazole). The eluted IL-7Rα was concentrated and passed over a Sephacryl S-200 (GE Healthcare) column equilibrated with TBS buffer. To recover properly refolded active receptor, IL-7Rα-HT was subsequently purified on an IL-7-coupled affinity column. The IL-7 affinity column was constructed by coupling ~20 mg purified IL-7 to CNBr-activated Sepharose resin (GE Healthcare) using amine chemistry through

lysine residues (Walsh *et al.*, 2004). The N-terminal His tag was cleaved by treating the IL-7Rα with biotinylated thrombin (Novagen) overnight at room temperature in TBS buffer. Biotinylated thrombin was removed by passage over strepavidin-coated beads (Novagen), while the cleaved His tag and uncleaved IL-7Rα-HT were removed by subsequent passage over a cobalt-affinity column. Mass spectrometry confirmed the molecular weights of the uncleaved and cleaved IL-7Rα ECD, as well as the formation of three disulfide bonds. Protein yields for refolded unglycosylated IL-7Rα were approximately 0.5–1 mg per litre of culture.

N-linked glycosylated IL-7Rα ECD was also produced in *Drosophila* Schneider 2 (S2) cells by cloning the gene into the pMT-BipA expression vector using the *Bgl*II and *Eco*RI restriction sites (Invitrogen). This expression vector secretes the protein into the culture medium after induction of the metallothionein promoter with copper. Stable S2 cell lines were generated by calcium phosphate cotransfection of the expression vectors with the blasticidin-resistant vector pCoBlast (Invitrogen). Blasticidin-resistant S2 cells were selected by growing the cells in Schneider's Complete Medium supplemented with 10% FBS and 25 µg ml^{-1} blasticidin S (Invitrogen). Large-scale protein expression was achieved after expansion and substitution into Insect-Xpress serum-free medium (Lonza) containing 20 m*M* L-glutamine and cells were induced with 700 µ*M* copper sulfate. Cells were harvested 6 d post-induction. Glycosylated IL-7Rα contained an N-terminal His tag followed by a thrombin protease-recognition sequence Arg-Ser-(His)$_6$-Ser-Ser-Gly-Leu-Val-Pro-Arg-Gly-Ser-His-Met. The cell-culture medium of each protein was concentrated using a tangential flow system, dialyzed against buffer *A* and purified as described previously for the cobalt-affinity column. The receptor was concentrated and passed over a Sephacryl S-200 column (GE Healthcare) as described above. The His tag was removed from the glycosylated IL-7Rα by thrombin cleavage and purification as detailed above, leaving a Gly-Ser-His-Met sequence at the N-terminus. Protein purity and glycosylation were confirmed by SDS–PAGE gel electrophoresis relative to unglycosylated protein produced by *E. coli*. Protein yields for the glycosylated IL-7Rα were approximately 15 mg per litre of cell culture.

A series of surface-loop mutations were constructed into the IL-7 gene using the QuikChange mutagenesis procedure (Stratagene). Three single and one double alanine mutations were introduced into the IL-7 sequence: E38A-IL-7, K111A-IL-7, E106A-IL-7 and E114A,E115A-IL-7. The surface-loop IL-7 variants were expressed in *E. coli* and purified to homogeneity with similar yields as described above for wt IL-7.

Selenomethionine (SeMet) incorporated E106A-IL-7 was generated by transformation of the expression vector into the *met*$^-$ *E. coli* BL21(DE3) CodonPlus RP-X cell strain (Stratagene). The cells were grown in M9 minimal media with amino acids and 50 mg l^{-1} L-selenomethionine (Sigma-Aldrich). SeMet-E106A-IL-7 was purified exactly as for the wt sequence described above. Mass spectroscopy indicates the incorporation of SeMet into 5–6 of the methionine sites.

Proteins produced from *E. coli* cells are designated (EC), while those from insect cells are designated (S2). Proteins produced from *E. coli* were unglycoslated and those expressed from insect cells were glycosylated.

2.2. Crystallization

For the unglycosylated complex, wt IL-7 and surface-loop IL-7 variants were mixed with IL-7Rα (EC), incubated overnight at 277 K and passed over a preparative size-exlusion chromatography (SEC) column (Sephacryl S-200 26/60, GE Healthcare) equilibrated in TBS buffer. The 1:1 unglycosylated protein complexes were concentrated to 4–5 mg ml^{-1}. The SeMet-E106A-IL-7–IL-7Rα (EC) complex was concentrated to 3 mg ml^{-1}. The same procedure was used for the complex of E106A-IL-7 with glycosylated IL-7Rα (S2, no His tag), except that 5 µl endoglycosidase H (Endo H, 2500 units, NEB) was added to the 4 mg ml^{-1} glycosylated protein complex solution without subsequent purification. In addition, fully glycosylated IL-7Rα (S2) complex with E106A-IL-7 was also tested at 4 mg ml^{-1} in TBS buffer. All protein-complex crystallization solutions were filtered through a 0.2 µm membrane and stored at 277 K.

Sparse-matrix crystal screening was performed using crystallization kits from Emerald Biostructures (Wizard Screens I, II and III) at 277, 292 and 310 K. Sitting-drop vapor-diffusion trials were set up using 0.5 ml reservoir solution with a drop consisting of 1 µl protein complex and 1 µl reservoir solution. Small protein crystals were observed at 292 K using various PEGs as the precipitating agent at around pH 6–8. Protein crystals were optimized by buffer refinement and microseeding. Microseeding involved removing small protein crystals into similar reservoir solution with an ∼5% excess of the precipitating agent. The small crystals were crushed using a Seed Bead kit (Hampton Research) and diluted tenfold. 1 µl of the diluted seed stocks was added to each sitting drop containing the soluble protein complex (1 µl) and reservoir solution (1 µl). All crystals were flash-frozen in liquid nitrogen by slowly increasing the glycerol concentration to 20% in the reservoir solution. A native X-ray data set of unglycosylated E106A-IL-7 (EC)–IL-7Rα (EC) was collected from a rod-shaped crystal with approximate dimensions 30 × 10 × 5 µm frozen in a 30 µm MiTeGen MicroMount. This crystal grew in 20% PEG 8000, 0.1 *M* MES pH 6.0 and 0.2 *M* calcium acetate. An X-ray data set was collected from a box-shaped crystal of the unglycosylated SeMet-E106A-IL-7Rα (EC) complex with approximate dimensions 20 × 10 × 10 µm in a 50 µm Hampton loop. Unglycosylated SeMet-protein crystals were obtained by microseeding the native complex crystals into the SeMet-complex drops

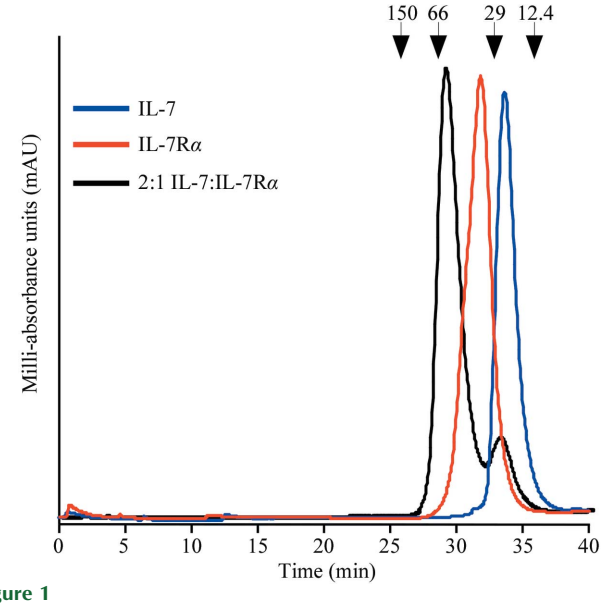

Figure 1
Analytical size-exclusion chromatography experiments on wt IL-7 (EC) and IL-7Rα (EC) ECD. A Superdex 200 10/300 GL SEC column (GE Healthcare) was equilibrated with PBS buffer pH 7.4 at a flow rate of 0.5 ml min^{-1} at 277 K. The blue chromatograph is an injection of 10 µ*M* IL-7 (EC) with a retention time of 33.7 min. The red chromatograph is an injection of 5 µ*M* IL-7Rα (EC) running at 31.8 min. The black chromatograph is an injection of a 2:1 molar ratio of IL-7 (EC):IL-7Rα (EC) with retention times of 29.8 and 33.6 min. The arrows above the chromatographs indicate the molecular weights of known standards.

Table 1
Data-collection statistics of the unglycosylated IL-7–IL-7Rα ECD complex.

Values in parentheses are for the highest resolution shell.

	Native	SeMet (λ_p, peak)	SeMet (λ_i, inflection)	SeMet (λ_r, remote)
Wavelength (Å)	0.97932	0.97929	0.97943	0.95662
Resolution (Å)	30–2.7 (2.8–2.7)	30–3.0 (3.11–3.0)	30–3.3 (3.42–3.3)	30–4.45 (4.45–4.3)
Unit-cell parameters				
a (Å)	47.2	46.9		
b (Å)	113.0	113.4		
c (Å)	87.5	87.1		
$\alpha = \gamma$ (°)	90.0	90.0		
β (°)	105.1	104.7		
Completeness (%)	88.2 (45.1)	97.2 (78.0)	91.3 (59.4)	90.2 (77.2)
Total reflections	71927	60779	39824	15548
Unique reflections	21610	17380	12459	5672
Average redundancy	3.3 (2.2)	3.5 (2.5)	3.2 (1.9)	2.7 (2.4)
R_{sym}† (%)	7.4 (34.0)	9.3 (28.8)	12.1 (32.3)	13.6 (28.7)
$I/\sigma(I)$	15.9 (2.1)	11.8 (2.7)	7.9 (1.8)	5.8 (2.7)
Space group	$P2_1$	$P2_1$	$P2_1$	$P2_1$

† $R_{sym} = \sum|I_h - \langle I_h\rangle|/\sum I_h$, where I_h is the measured intensity for an individual reflection and $\langle I_h\rangle$ is the average intensity for that reflection.

using the following conditions: 16% PEG 8000, 0.1 *M* MES pH 6.0 and 0.2 *M* calcium acetate. Glycosylated protein crystals of the E106A-IL-7–IL-7Rα (S2) complex grew from 18% PEG 3350, 0.1 *M* HEPES pH 7.4, 0.2 *M* NaCl with microseeding. A native glycosylated 1:1 complex X-ray data set was collected from a frozen crystal with approximate dimensions 50 × 40 × 10 µm in a 50 µm Hampton loop.

2.3. Data collection

All X-ray diffraction data were collected at Structural Biology Center (SBC) beamline 19ID, Advanced Photon Source, Argonne National Laboratory, Chicago, IL, USA. Owing to the small size of the protein crystals, the X-ray beam was collimated to an area of 50 µm^2 and diffraction data were recorded with an ADSC Quantum 315 CCD detector at 100 K. For the unglycosylated E106A-IL-7–IL-7Rα (EC) complex, X-ray diffraction data were collected with 2 s exposures for 1° oscillations for a total of 180° at a wavelength of 0.97932 Å. A selenium X-ray fluorescence scan was recorded on an unglycosylated SeMet-E106A-IL-7–IL-7Rα (EC) protein crystal to determine the appropriate wavelengths. A three-wavelength MAD data set was collected at peak, inflection and remote wavelengths using 4 s exposure for 1° oscillations for a total of 180°. The glycosylated E106A-IL-7–IL-7Rα (S2) X-ray data-collection strategy used a 5 s exposure for 1° oscillations for a total of 120° at a wavelength of 0.97888 Å. Data were integrated and scaled using *HKL*-2000 (Otwinowski & Minor, 1997). X-ray data-collection statistics are presented in Tables 1 and 2.

3. Results and discussion

Wild-type IL-7 bound to unglycosylated or glycosylated IL-7Rα ECD in a 1:1 assembly as determined by size-exclusion chromatography experiments (Fig. 1). Injection of free IL-7 (EC) or IL-7Rα (EC) resulted in peaks with retention times of 33.7 min (IL-7, blue trace) and 31.8 min (IL-7Rα, red trace), respectively. When the proteins were mixed in a 1:1 (data not shown) or 2:1 molar ratio (black trace) of IL-7 to IL-7Rα, a peak with a shorter retention time of 29.8 min appeared, corresponding to a species with an apparent molecular weight of 50 kDa. The 1:1 complex has a predicted molecular weight of 45 kDa. Over-titration with IL-7 (2:1 molar ratio) shows another peak corresponding to free unbound IL-7 (33.6 min). Fractions were collected from each SEC experiment and the samples were run on SDS–PAGE gels to confirm the species present in each chromatography peak (data not shown). The shorter retention peak of 29.8 min corresponds to the 1:1 complex IL-7–IL-7Rα. wt IL-7 (EC) and the surface-loop variants also associate with glycosylated IL-7Rα (S2) in a 1:1 stoichiometry (data not shown).

Optimized protein crystals of the unglycosylated wt IL-7 (EC)–IL-7Rα (EC) complex diffracted to ∼5 Å at the synchrotron. Therefore, the surface-loop entropy-reduction approach described by Derewenda and coworkers was used to engineer alanine mutations into surface-exposed glutamates and/or lysines of the IL-7 sequence (Derewenda, 2004; Cooper *et al.*, 2007). A homology model of IL-7 guided the mutagenesis strategy for residues outside the predicted binding interface with the IL-7Rα ECD (Cosenza *et al.*, 2000). Three single and one double alanine mutations were introduced into the IL-7 sequence: E38A-IL-7, K111A-IL-7, E106A-IL-7 and E114A, E115A-IL-7. These IL-7 variants formed a 1:1 complex with the unglycosylated IL-7Rα and yielded protein crystals. The E38A-IL-7, K111A-IL-7 and E114A,E115A-IL-7 unglycosylated receptor complex crystals diffracted to ∼5, 4 and 4 Å, respectively.

A protein crystal of the unglycosylated receptor in complex with the E106A-IL-7 variant diffracted to 2.7 Å (Figs. 2*a* and 2*c*) and the data-collection statistics are listed in Table 1. The data from this crystal were processed in the monoclinic space group $P2_1$, with unit-

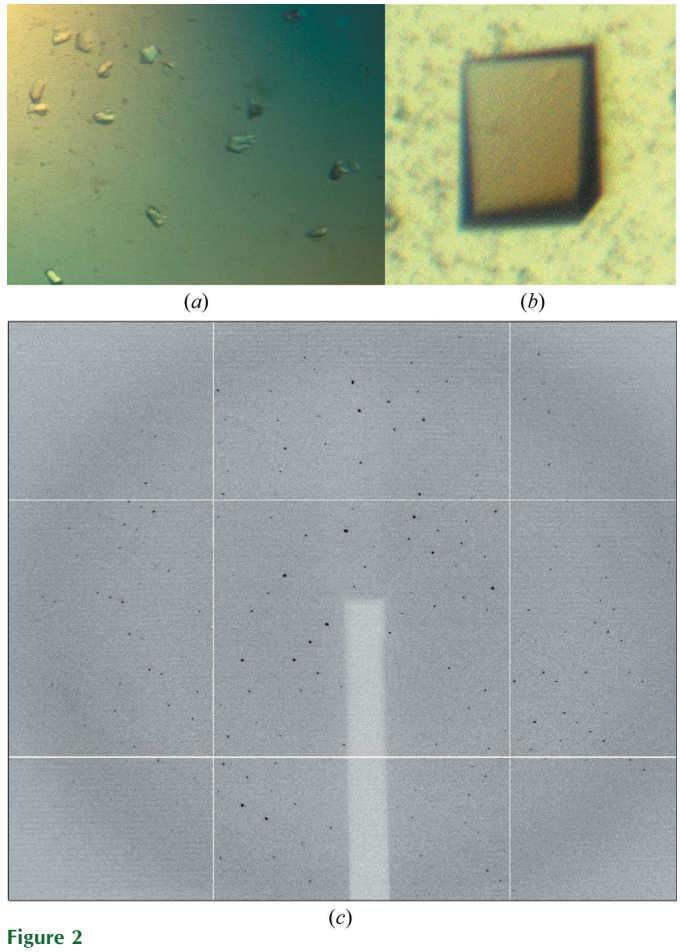

Figure 2
Crystals of the 1:1 complexes of E106A-IL-7 with unglycosylated and glycosylated IL-7Rα ECD. (*a*) Small rod-shaped protein crystals of the unglycosylated E106A-IL-7–IL-7Rα (EC) ECD complex with dimensions of <40 µm in all dimensions. (*b*) Prism-shaped protein crystal of the complex of E106A-IL-7 with glycosylated IL-7Rα (S2) ECD with dimensions of approximately of 50 × 40 × 10 µm. (*c*) Native X-ray diffraction image of a unglycosylated E106A-IL-7–IL-7Rα (EC) ECD complex crystal with diffraction to 2.7 Å.

Table 2
Data-collection statistics of a glycosylated IL-7–IL-7Rα ECD complex.

Values in parentheses are for the highest resolution shell.

Wavelength (Å)	0.97888
Resolution (Å)	30–3.0 (3.12–3.0)
Total reflections	35183
Unique reflections	8405
Average redundancy	4.0 (2.1)
Completeness (%)	92.6 (62.6)
R_{sym}† (%)	5.3 (34.3)
$I/\sigma(I)$	19.8 (2.2)
Space group	$P2_12_12_1$
Unit-cell parameters (Å, °)	a = 55.6, b = 68.2, c = 112.3, $\alpha = \beta = \gamma = 90$

† $R_{sym} = \sum|I_h - \langle I_h\rangle|/\sum I_h$, where I_h is the measured intensity for an individual reflection and $\langle I_h\rangle$ is the average intensity for that reflection.

cell parameters a = 47.2, b = 113.0, c = 87.5 Å, β = 105.1°. Two full interleukin–α-receptor complexes in the asymmetric unit yield a Matthews coefficient (V_M) of 2.65 Å^3 Da^{-1}, with 54% solvent content. Analysis of the self-rotation function of the data using *MOLREP* (Vagin & Teplyakov, 1997) reveals twofold noncrystallographic symmetry nearly coincident with the crystallographic twofold.

The E106A-IL-7 surface-loop variant bound to glycosylated IL-7Rα (S2) produced from insect cells and yielded needle crystals that diffracted to ∼6 Å at the synchrotron. To potentially reduce the inherent flexibility of the glycans and to improve diffraction, the glycosylated E106A-IL-7 (EC)–IL-7Rα (S2) complex was reacted with endoglycosidase H (Endo H). Endo H cleaves the glycosidic bond between the first two *N*-acetyl glucosamines (GlcNAc), leaving only the proximal GlcNAc attached to the asparagine. This enzymatic treatment resulted in prism-shaped crystals (Fig. 2*b*) that diffracted to atomic resolution (Table 2). The glycosylated crystal belonged to the orthorhombic space group $P2_12_12_1$, with one IL-7–α-receptor complex in the asymmetric unit (V_M = 2.52 Å^3 Da^{-1}) and a solvent content of 51%.

Attempts to solve the crystal structure of either the unglycosylated or glycosylated IL-7–α-receptor complexes using molecular replacement with known structures of related hematopoietic cytokines and/or receptors as models failed to produce unique phasing solutions. Therefore, selenomethionine was incorporated into E106A-IL-7 and this was then added to unglycosylated IL-7Rα (EC) to form the unglycosylated SeMet complex. A three-wavelength MAD data set was collected from the unglycosylated SeMet complex (Table 1). The unglycosylated SeMet complex belongs to space group $P2_1$, with similar unit-cell parameters to those of the native unglycosylated complex. The structure of the unglycosylated complex will be solved using traditional MAD (Hendrickson & Ogata, 1997) or SAD (de La Fortelle & Bricogne, 1997; González, 2003) methodologies. Molecular replacement (Rossmann, 2001) using the unglycosylated complex structure as a model will be used to solve the glycosylated complex structure.

We thank Dr Julie Dohm for critical reading of the manuscript. We thank Dr Apostolos Gittis for crystallography advice. The X-ray data were collected using the Structural Biology Center (SBC) 19ID beamline at the Advanced Photon Source at Argonne National Laboratory, which is operated by UChicago Argonne LLC for the US Department of Energy, Office of Biological and Environmental Research under contract DE-AC02-06CH11357. We thank Drs Stephan Ginell, Youngchang Kim, Frank Rotella, Krzysztof Lazarski and Marianne Cuff of the SBC staff for their assistance and discussions. This research was supported by grant 0535131N from the American Heart Association National Center.

References

Bazan, J. F. (1990). *Proc. Natl Acad. Sci. USA*, **87**, 6934–6938.
Cooper, D. R., Boczek, T., Grelewska, K., Pinkowska, M., Sikorska, M., Zawadzki, M. & Derewenda, Z. (2007). *Acta Cryst.* D**63**, 636–645.
Cosenza, L., Rosenbach, A., White, J. V., Murphy, J. R. & Smith, T. (2000). *Protein Sci.* **9**, 916–926.
Cosenza, L., Sweeney, E. & Murphy, J. R. (1997). *J. Biol. Chem.* **272**, 32995–33000.
Damas, J. K., Waehre, T., Yndestad, A., Otterdal, K., Hognestad, A., Solum, N. O., Gullestad, L., Froland, S. S. & Aukrust, P. (2003). *Circulation*, **107**, 2670–2676.
Derewenda, Z. S. (2004). *Structure*, **12**, 529–535.
Digel, W., Schmid, M., Heil, G., Conrad, P., Gillis, S. & Porzsolt, F. (1991). *Blood*, **78**, 753–759.
Fry, T. J. & Mackall, C. L. (2002). *Blood*, **99**, 3892–3904.
González, A. (2003). *Acta Cryst.* D**59**, 315–322.
Goodwin, R. G., Friend, D., Ziegler, S. F., Jerzy, R., Falk, B. A., Gimpel, S., Cosman, D., Dower, S. K., March, C. J., Namen, A. E. & Park, L. S. (1990). *Cell*, **60**, 941–951.
Goodwin, R. G., Lupton, S., Schmierer, A., Hjerrild, K. J., Jerzy, R., Clevenger, W., Gillis, S., Cosman, D. & Namen, A. E. (1989). *Proc. Natl Acad. Sci. USA*, **86**, 302–306.
Grabstein, K. H., Waldschmidt, T. J., Finkelman, F. D., Hess, B. W., Alpert, A. R., Boiani, N. E., Namen, A. E. & Morrissey, P. J. (1993). *J. Exp. Med.* **178**, 257–264.
Hage, T., Sebald, W. & Reinemer, P. (1999). *Cell*, **97**, 271–281.
Harada, S., Yamamura, M., Okamoto, H., Morita, Y., Kawashima, M., Aita, T. & Makino, H. (1999). *Arthritis Rheum.* **42**, 1508–1516.
Hendrickson, W. A. & Ogata, C. M. (1997). *Methods Enzymol.* **276**, 494–523.
Ji, R. C. (2006). *Lymphat. Res. Biol.* **4**, 83–100.
Jiang, Q., Li, W. Q., Aiello, F. B., Mazzucchelli, R., Asefa, B., Khaled, A. R. & Durum, S. K. (2005). *Cytokine Growth Factor Rev.* **16**, 513–533.
Khaled, A. R. & Durum, S. K. (2003). *Immunol. Rev.* **193**, 48–57.
Kroemer, R. T., Doughty, S. W., Robinson, A. J. & Richards, W. G. (1996). *Protein Eng.* **9**, 493–498.
Kroemer, R. T., Kroncke, R., Gerdes, J. & Richards, W. G. (1998). *Protein Eng.* **11**, 31–40.
Kroemer, R. T. & Richards, W. G. (1996). *Protein Eng.* **9**, 1135–1142.
La Fortelle, E. de & Bricogne, G. (1997). *Methods Enzymol.* **276**, 472–494.
Leonard, W. J. (2002). *Nature Immunol.* **3**, 605–607.
Levine, S. J. (2004). *J. Immunol.* **173**, 5343–5348.
Lupton, S. D., Gimpel, S., Jerzy, R., Brunton, L. L., Hjerrild, K. A., Cosman, D. & Goodwin, R. G. (1990). *J. Immunol.* **144**, 3592–3601.
Ma, A., Koka, R. & Burkett, P. (2006). *Annu. Rev. Immunol.* **24**, 657–679.
Merle-Beral, H., Schmitt, C., Mossalayi, D., Bismuth, G., Dalloul, A. & Mentz, F. (1993). *Nouv. Rev. Fr. Hematol.* **35**, 231–232.
Morrissey, P. J., Goodwin, R. G., Nordan, R. P., Anderson, D., Grabstein, K. H., Cosman, D., Sims, J., Lupton, S., Acres, B. & Reed, S. G. (1989). *J. Exp. Med.* **169**, 707–716.
Otwinowski, Z. & Minor, W. (1997). *Methods Enzymol.* **276**, 307–326.
Ozaki, K. & Leonard, W. J. (2002). *J. Biol. Chem.* **277**, 29355–29358.
Pandey, A., Ozaki, K., Baumann, H., Levin, S. D., Puel, A., Farr, A. G., Ziegler, S. F., Leonard, W. J. & Lodish, H. F. (2000). *Nature Immunol.* **1**, 59–64.
Plas, D. C. van der, Smiers, F., Pouwels, K., Hoefsloot, L. H., Lowenberg, B. & Touw, I. P. (1996). *Leukemia*, **10**, 1317–1325.
Ponda, P., Schuval, S. J., Kaplan, B., Logalbo, P., Roberts, J. L. & Bonagura, V. R. (2006). *Ann. Allergy Asthma Immunol.* **97**, 755–758.
Puel, A., Ziegler, S. F., Buckley, R. H. & Leonard, W. J. (1998). *Nature Genet.* **20**, 394–397.
Rochman, I., Watanabe, N., Arima, K., Liu, Y. J. & Leonard, W. J. (2007). *J. Immunol.* **178**, 6720–6724.
Rossmann, M. G. (2001). *Acta Cryst.* D**57**, 1360–1366.
Sfikakis, P. P. & Tsokos, G. C. (1995). *Clin. Exp. Rheumatol.* **13**, 763–777.
Vagin, A. & Teplyakov, A. (1997). *J. Appl. Cryst.* **30**, 1022–1025.
Vos, A. M. de, Ultsch, M. & Kossiakoff, A. A. (1992). *Science*, **255**, 306–312.
Walsh, S. T., Sylvester, J. E. & Kossiakoff, A. A. (2004). *Proc. Natl Acad. Sci. USA*, **101**, 17078–17083.
Watanabe, M., Ueno, Y., Yajima, T., Okamoto, S., Hayashi, T., Yamazaki, M., Iwao, Y., Ishii, H., Habu, S., Uehira, M., Nishimoto, H., Ishikawa, H., Hata, J. & Hibi, T. (1998). *J. Exp. Med.* **187**, 389–402.
Woldbaek, P. R., Hoen, I. B., Christensen, G. & Tonnessen, T. (2002). *Acta Physiol. Scand.* **175**, 173–181.